

## Effect of Resonances on the Coherent Control of the Photoionization and Photodissociation of HI and DI

Langchi Zhu,<sup>1</sup> Kunihiro Suto,<sup>2</sup> Jeanette Allen Fiss,<sup>1</sup> Ryuichi Wada,<sup>2</sup> Tamar Seideman,<sup>3,\*</sup> and Robert J. Gordon<sup>1</sup>

<sup>1</sup>Department of Chemistry (m/c 111), University of Illinois at Chicago, 845 W Taylor Street, Chicago, Illinois 60607-7061

<sup>2</sup>Department of Molecular Engineering, Kyoto University, Kyoto 60601, Japan

<sup>3</sup>Institute for Theoretical Atomic and Molecular Physics, Harvard-Smithsonian Center for Astrophysics, 60 Garden Street, Cambridge, Massachusetts 02138

(Received 21 May 1997)

The phase lag between the ionization and dissociation products of HI and DI molecules obtained by one- and three-photon excitation was measured as a function of excitation energy in the vicinity of a molecular resonance. The phase lag was observed to have an asymmetric profile with a deep minimum near the center of the resonance. A strong isotope effect was also observed. A theoretical analysis, using projection operators to partition the Lippmann-Schwinger equation, showed that a molecular phase is responsible for the energy dependence of the phase lag. [S0031-9007(97)04599-7]

PACS numbers: 33.80.Rv, 32.80.Qk, 82.50.Fv

Controlling the branching ratios of atomic and molecular processes by quantum mechanical interference has received much recent attention [1,2]. Control has been achieved in various experiments by using two excitation paths to populate a continuum state and varying either the energy detunings or the relative phase of the two paths. An example of the first method is a three-level  $\Lambda$  excitation scheme to induce structure in the continuum of Na<sub>2</sub> [3]. One laser was used to transfer population to the continuum, while a second, more intense laser was used to drive a transition from an unpopulated level to the continuum. The control parameter in this case is the energy difference between the final states reached by the two paths. A second example is the use of a four-level diamond configuration to reach a common upper level of Ba via two different resonant states [4]. The control parameter in this case is the detuning from the intermediate states. In both experiments, control is achieved by using energy tuning to alter the profile of a continuum state, which in turn affects the dissociation or ionization product ratio [5]. The phases of the two paths play no role in these experiments.

A different control strategy is to fix the energies and vary the relative phase of the two paths. For example, the two paths may consist of excitation from a discrete initial state to a degenerate continuum by either three photons of frequency  $\omega_1$  (wavelength  $\lambda_1$ ) or by one photon of frequency  $\omega_3 = 3\omega_1$  [6]. The excited continuum state correlates asymptotically to two product channels, A and B. The probability of forming product channel S by a single photon is  $p_3^S = I_3 F_3^S$ , whereas the probability of obtaining the same product channel by three photons is  $p_1^S = I_1^3 F_1^S$ , where  $I_3$  and  $I_1$  are the intensities of the two laser beams, and  $F_3^S$  and  $F_1^S$  are frequency-dependent constants. When both fields are present, the total probability of forming each product channel is [6]

$$p^S = p_1^S + p_3^S + 2(I_3 I_1^3)^{1/2} |F_{13}^S| \cos(\phi + \delta_{13}^S), \quad (1)$$

where  $F_{13}^S$  is a frequency dependent constant, and  $\phi =$

$\phi_3 - 3\phi_1$  is the phase difference of the two fields. We define the phase lag of the two channels by the difference  $\Delta\delta = \delta_{13}^A - \delta_{13}^B$ . The yield of product channel S can be maximized (or minimized) by setting  $\phi = -\delta_{13}^S$ . The physical origin of  $\delta_{13}^S$  will be discussed later.

Recently Zhu *et al.* [7] reported using this scheme to control the branching ratio of ionization and dissociation of HI molecules at energies slightly above the first ionization potential ( $\sim 10.6$  eV). The principle finding of that study was that at wavelengths  $\lambda_1$  near 355 nm  $\Delta\delta$  was  $\sim 150^\circ$ , whereas for  $\lambda_1$  near 354 nm  $\Delta\delta$  was  $\sim 0$ . Although the source of the phase lag was unknown, the observation that the two wavelength regions correspond to transitions to different molecular Rydberg states suggests that resonances might play a role in the energy dependence of  $\Delta\delta$ . We report here data and theory which clarify the control mechanism.

The experimental method has been described previously [8]. Briefly, a pulsed (10 Hz) molecular beam of HI or DI was injected between repeller and extractor electrodes in a vacuum chamber. The molecular beam was crossed with a XeCl excimer-pumped UV dye laser (4 mJ/pulse). The third harmonic of the dye laser was generated by focusing the laser beam into a cell containing 2–10 Torr of Xe. The phase between the fundamental (UV) and the vacuum ultraviolet (VUV) third harmonic was varied by passing the two beams through a chamber containing several Torr of H<sub>2</sub> gas, which has very different refractive indices at the two wavelengths [9]. The two beams were focused into the reaction chamber by a pair of Al/MgF<sub>2</sub>-coated spherical mirrors ( $f = 20.3$  cm). Ions produced in the reaction region were accelerated into a 1 m flight tube and detected by a microchannel plate and a boxcar signal averager. HI<sup>+</sup> (or DI<sup>+</sup>) and I<sup>+</sup> mass peaks were monitored as the H<sub>2</sub> pressure was slowly increased, so that  $\phi$  varied by at least five cycles of  $2\pi$ . From previous work [7,10] we know that the I<sup>+</sup> peak is produced by the ionization of neutral I atoms by one or more  $\omega_1$

photons. Typical data are shown in Fig. 1, displaying modulation of the  $\text{DI}^+$  and  $\text{I}^+$  signals. The VUV laser intensity was adjusted so that the one- and three-photon signals were nearly equal. The pressure scans were fit to a sinusoidal function, and  $\Delta\delta$  was determined from the phase difference between the molecular and atomic ion signals.

The goal of the present study is to measure and rationalize the energy dependence of  $\Delta\delta$  in the vicinity of an autoionizing and predissociating resonance. We chose to study the  $(X^2\Pi_{1/2})5s\sigma(v=0)$  resonance of HI and DI, which is centered near  $\lambda_1 = 354.0$  nm ( $\lambda_3 = 118.0$  nm) [11–13]. First we measured the effects of the individual laser fields. Figure 2 shows the one-photon (VUV) and three-photon (UV) molecular and atomic ion spectra recorded for each molecule. The VUV spectra were obtained by focusing both beams into the chamber with a  $\text{MgF}_2$  lens ( $f \approx 12.5$  cm at 118 nm). This lens was positioned so that only the VUV beam overlapped the molecular beam within the field of view of the detector. In order to ionize the I atom fragment, a 355 nm laser beam (the third harmonic of a Nd:YAG laser) was made to overlap the VUV beam by focusing it with a 10 cm quartz lens. No ions were detected in the one-photon spectra without Xe in the tripling cell, and no  $\text{I}^+$  was detected without the 355 nm laser. The UV spectra were taken using a quartz lens to focus only the UV radiation (4 mJ/pulse,  $f = 7.6$  cm) into the chamber.

The  $5s\sigma$  resonance is apparent in all of the spectra. The oscillatory structure in the vicinity of the resonance is of rotational origin [13]. The rising edge of the  $5f\sigma/5f\pi$  resonances appears in the VUV spectra on the low energy side of the  $5s\sigma$  resonance. In the UV spectra, the rising signal on the high energy side of the  $5s\sigma$  resonance is caused by two-photon excitation of the  $b^3\Pi_1$  Rydberg state [7]. Predissociation of this state produces I atoms, whereas absorption of a third photon leads to  $2 + 1$  resonance-enhanced multiphoton ionization of the parent molecule. The periodic oscillations on the blue side of

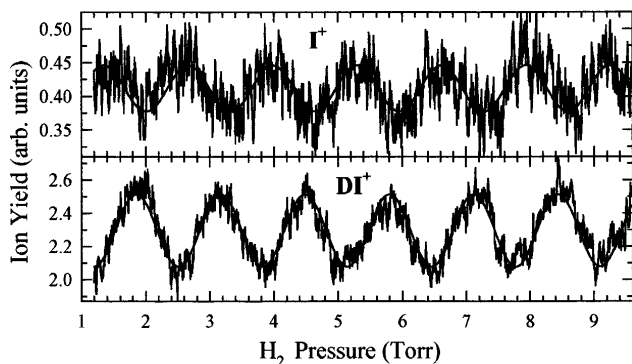


FIG. 1. Modulation curves for  $\text{DI}^+$  and  $\text{I}^+$  recorded at  $\lambda_1 = 353.69$  nm.

the UV spectra are from the tail of the O branch of the two-photon  $b^3\Pi_1 \leftarrow X^1\Sigma^+$  transition.

The principal results of this study, obtained with both lasers present, are shown in Fig. 3. The phase lag between the two reaction channels was measured at 0.05 nm intervals of  $\lambda_1$  between 353.44 and 354.24 nm for both HI and DI. At least ten scans were recorded at each wavelength. The data for the two isotopomers display a number of striking similarities and differences. The phase lag for both molecules has a minimum near the center of the  $5s\sigma$  resonance and increases asymmetrically on either side. The phase lag for HI, however, is much broader and has a deeper minimum for ( $10^\circ$  vs  $30^\circ$ ) which is shifted to the red of the DI minimum. It is evident that the  $5s\sigma$  resonance plays an important role in the control mechanism.

In our earlier work [7] the origin of the phase lag and its strong energy dependence were unclear, and different explanations have been suggested in the recent literature [14–16]. To gain insight into the origin and potential implications of the observed phase lag we developed a fully nonperturbative model based on partitioning of the solution of the Lippmann-Schwinger equation [17] corresponding to the complete Hamiltonian  $H = H_M + D^{(1)} + D^{(3)}$ , where  $H_M$  is the matter Hamiltonian, and  $D^{(j)}$  is a  $j$ -photon transition dipole operator [18]. Only a

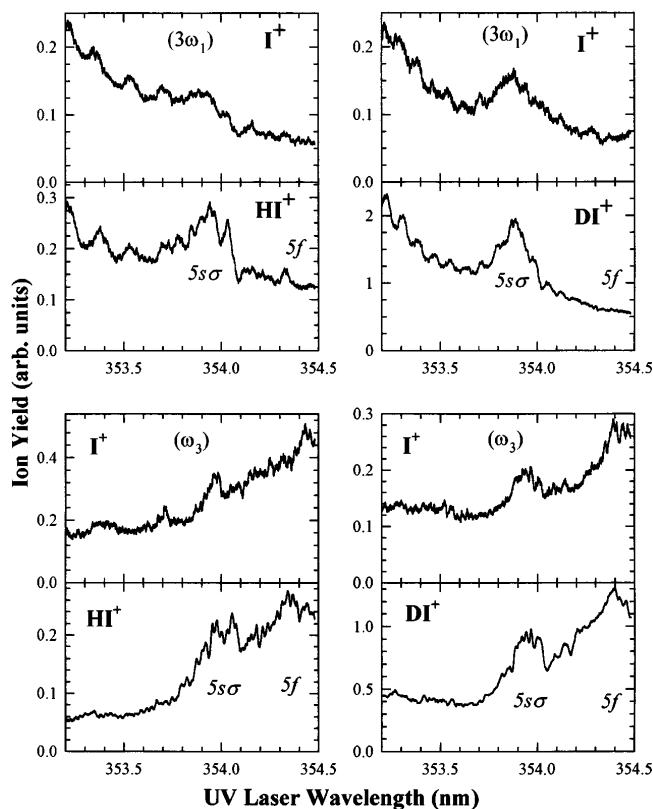


FIG. 2. One- and three-photon spectra of atomic and molecular ions produced from HI and DI.

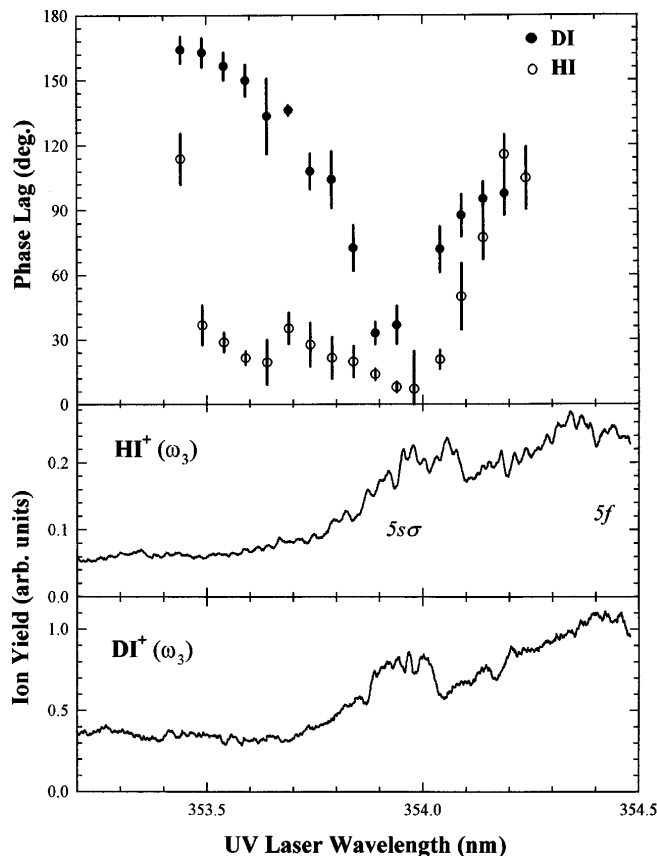


FIG. 3. Phase lag between the dissociation and ionization channels for HI (open symbols) and DI (closed symbols). The VUV ionization spectra of HI and DI are shown in the bottom panels.

brief outline is presented below, where, for simplicity of presentation, we treat the field-matter interaction within the golden rule approximation. We consider a bound eigenstate  $|g\rangle$  that is coupled to several continua of general nature, both directly and via a manifold of (possible coupled) resonances (see Fig. 4).

Following partitioning of the eigenstates  $|ES\hat{k}^- \rangle$  of the field free Hamiltonian  $H_M$  we obtain for the matrix element of  $D^{(j)}$

$$\begin{aligned} \langle g|D^{(j)}|ES\hat{k}^- \rangle &= \langle g|D^{(j)}|ES\hat{k}_1^- \rangle \\ &+ \langle g|D^{(j)}[I + (E^- - PH_M P)^{-1}PH_M] \\ &\times QGQH_M|ES\hat{k}_1^- \rangle, \end{aligned} \quad (2)$$

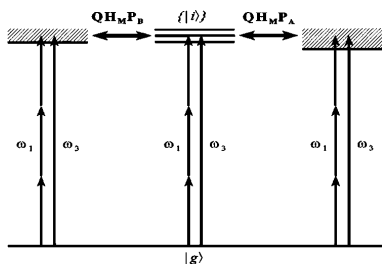


FIG. 4. Schematic drawing of the model.

where  $E$  is the total energy, and  $\hat{k}$  denotes the photofragment or photoelectron scattering angles. In Eq. (2) the  $-$  superscript signifies incoming wave boundary conditions, serving as a reminder that  $|ES\hat{k}^- \rangle$  evolves in the limit where the unbound coordinate  $q^S$  [the internuclear separation vector in the case of (pre)dissociation and the electron-core separation vector in the case of (auto)ionization] approaches infinity to an eigenstate of an asymptotic Hamiltonian  $\lim_{q^S \rightarrow \infty} H_M$ , with well-defined channel index  $S$  and scattering angles  $\hat{k}$ . We denote by  $P$  a joint projector onto the continua,  $P = \sum_S P_S$  with  $P_S H P_{S'} = 0$  for  $S' \neq S$  and  $Q|ES\hat{k}^- \rangle$  is the portion of the eigenstate that vanishes asymptotically. Thus,  $P_S H_M P_S$  is the scattering Hamiltonian of the uncoupled  $S$  continuum,  $|ES\hat{k}_1^- \rangle$  are the eigenstates of  $P_S H_M P_S$ ,  $P_S H_M Q$  is the nonadiabatic interaction coupling the excited and continuum manifolds, and  $QGQ = [E^- - Q\mathcal{H}Q]^{-1}$  is the Green operator corresponding to an effective Hamiltonian  $Q\mathcal{H}Q = QH_M Q + QH_M P(E^- - PH_M P)^{-1}PH_M Q$  (see Fig. 4). The extension of this formalism to the case of a nonperturbative field and details of the theory will be published separately [18].

Constructive and destructive interference between the direct (first) and resonance-mediated (second) terms of Eq. (2) produce a Fano-type line shape [19] for both the one- and three-photon processes [ $p_1^S$  and  $p_3^S$  in Eq. (1)]. The total transition probability for channel  $S$  is given by

$$p^S = |\langle g|D^{(1)}|ES\hat{k}^- \rangle + e^{i\phi} \langle g|D^{(3)}|ES\hat{k}^- \rangle|^2, \quad (3)$$

which has the same form as Eq. (1). The origin of the phase lag may be seen explicitly by identifying the phase of each of the terms in Eq. (2). The direct amplitude can be written as  $f_j^{S,d} \exp(i\delta_j^{S,d}) = \langle g|D^{(j)}|ES\hat{k}_1^- \rangle$  where  $f_j^{S,d}$  and  $\delta_j^{S,d}$  are real. Assuming first that a single resonance dominates,  $Q = |i\rangle\langle i|$ , the resonance-mediated amplitude can be written as the product of two factors,  $f_j^{S,r} \exp(i\delta_j^{S,r}) = \langle g|D^{(j)}[(E^- - PH_M P)^{-1}PH_M + I]|i\rangle\langle i|H_M|ES\hat{k}_1^- \rangle$  and  $f \exp(i\delta) = [E - E_i - \Delta_i - i\Gamma_i/2]^{-1}$ , where  $E_i$  is the eigenvalue of  $QH_M Q$  corresponding to eigenvector  $|i\rangle$ , and  $\Gamma_i$  and  $\Delta_i$  are the standard width and shift parameters [17] (modified to account for the presence of two continua [18]). The quantity  $\delta$  is the familiar Breit-Wigner phase [20], and  $\delta_j^{S,d}$  and  $\delta_j^{S,r}$  may be described as ‘‘molecular phases,’’ which arise from the fact that  $|ES\hat{k}_1^- \rangle$  is complex. Another possible source of the molecular phase is a continuum intermediate state in the three-photon process [16]. With the above definitions the transition probability for channel  $S$  takes the form

$$\begin{aligned} p^S &= |f_1^{S,d} e^{i\delta_1^{S,d}} + f_1^{S,r} f e^{i(\delta_1^{S,r} + \delta)} \\ &+ e^{i\phi} (f_3^{S,d} e^{i\delta_3^{S,d}} + f_3^{S,r} f e^{i(\delta_3^{S,r} + \delta)})|^2. \end{aligned} \quad (4)$$

Several limiting forms of this equation are apparent, giving rise to different schemes for controlling the product branching ratio. One scheme may be achieved by

scanning a single laser across the resonance (e.g., by setting  $f_1^{S,d} = f_1^{S,r} = 0$  and varying  $\delta$ ) [21]. Control is possible because the relative flux into each channel depends on the interference between the direct and indirect paths, which varies with excitation energy. Another, more active form of control results from interference between the one- and three-photon paths. Control is achieved at a fixed energy by selecting  $\phi$  to maximize the flux in either channel. The phase lag can arise from two sources. The first shown by Nakajima *et al.* [15,22] is a consequence of the fact that the shape of the Fano profile in a bichromatic field depends on the phase difference  $\phi$  of the two fields. It follows from their work that the cross term in Eq. (1) can have a nonvanishing value of  $\delta_{13}^S$  even if the molecular phases are all zero. In this case, however, one can show [18] that  $\delta_{13}^S \rightarrow 0$  far from resonance, whereas the experimental phase lag has a minimum near resonance and rises strongly far from the center of the resonance.

The second source of  $\Delta\delta$  is the molecular phase. From Eqs. (2) and (4) we find that, in the limit of a single resonance and no direct component, the molecular phase vanishes. With the first term of Eq. (2) omitted,  $p_1^S$  and  $p_3^S$  take Lorentzian line shapes, and the cross term

$$F_{13}^S = \int d\hat{k} \times \frac{\langle g|D^{(1)}|i\rangle\langle i|H_M|ES\hat{k}_1^-\rangle\langle ES\hat{k}_1^-|H_M|i\rangle\langle i|D^{(3)}|g\rangle}{(E - E_i - \Delta_i)^2 + (\Gamma_i/2)^2} \quad (5)$$

is real. In the presence of a direct component  $F_{13}^S$  includes three additional terms, of which the product of the two direct components of the one- and three-photon elements dominates far from resonance, while the product of the resonant components, Eq. (5), dominates on resonance. Provided the direct component carries an at most weakly energy dependent molecular phase,  $\delta_{13}^S$  has a minimum on resonance and rises asymmetrically as the frequency is red or blue detuned, saturating at the value corresponding to the direct process alone far from the resonance, as indeed was observed experimentally (Fig. 3). More generally, if several resonances contribute,  $F_{13}^S$  is no longer real and the energy dependence of the phase lag is more structured. The qualitative behavior of the phase is, nevertheless, similar, having minima at the resonance energies and rising to the asymptotic plateau. A nonnegligible direct component and/or overlapping resonances would produce a net phase also on resonance [18].

In conclusion, we have shown that the phase lag between dissociation and ionization is caused by a molecular phase, and that the energy dependence of the phase lag is caused by a resonance coupled to two continua. In the center of the resonance the molecular phase for the one- and three-photon paths nearly cancels, producing a minimum in the phase lag. In this region the phase in-

formation contained in the preparation step is lost in the eventual decay of the molecule. Off resonance, the phase lag can be used to determine the relative phase of two outgoing wave functions, a quantity not readily obtained by other methods. Moreover, our experimental data and theoretical formalism point to the possibility of determining resonance lifetimes by measurement of the phase lag, even in the presence of a direct component.

We wish to thank Dr. H. Lefebvre-Brion and Professor S. Lee for many stimulating discussions. Support by the NSF and the JSPS is gratefully acknowledged. T.S. thanks the NSF for support through a grant to ITAMP at Harvard University.

---

\*Permanent address: Steacie Institute, National Research Council, 100 Sussex Drive, Ottawa K1A0R6, Canada.

- [1] R. J. Gordon and S. A. Rice, *Annu. Rev. Phys. Chem.* **48**, 595 (1997).
- [2] W. S. Warren, H. Rabitz, and M. Dahleh, *Science* **269**, 1581 (1993).
- [3] A. Shnitman, I. Sofer, I. Golub, A. Yogeve, M. Shapiro, Z. Chen, and P. Brumer, *Phys. Rev. Lett.* **76**, 2886 (1996).
- [4] F. Wang, C. Chen, and D. S. Elliott, *Phys. Rev. Lett.* **77**, 2416 (1996).
- [5] S. T. Pratt, *J. Chem. Phys.* **104**, 5776 (1996).
- [6] M. Shapiro, J. W. Hepburn, and P. Brumer, *Chem. Phys. Lett.* **149**, 451 (1988).
- [7] L. Zhu, V. Kleiman, X. Li, S. Lu, K. Trentelman, and R. J. Gordon, *Science* **270**, 77 (1995).
- [8] S. Lu, S. M. Park, Y. Xie, and R. J. Gordon, *J. Chem. Phys.* **96**, 6613 (1992).
- [9] R. J. Gordon, S. Lu, S. M. Park, K. Trentelman, Y. Xie, L. Zhu, A. Kumar, and W. J. Meath, *J. Chem. Phys.* **98**, 9481 (1993).
- [10] V. D. Kleiman, L. Zhu, J. Allen, and R. J. Gordon, *J. Chem. Phys.* **103**, 10 800 (1995).
- [11] J. H. D. Eland and J. Berkowitz, *J. Chem. Phys.* **67**, 5034 (1977).
- [12] D. J. Hart and J. W. Hepburn, *Chem. Phys.* **129**, 51 (1989).
- [13] A. Mank, M. Drescher, T. Huthe-Fehre, N. Böwering, U. Heinzemann, and H. Lefebvre-Brion, *J. Chem. Phys.* **95**, 1676 (1991).
- [14] H. Lefebvre-Brion, *J. Chem. Phys.* **106**, 2544 (1997).
- [15] T. Nakajima, J. Zhang, and P. Lambropoulos, *J. Phys. B* **30**, 1077 (1997).
- [16] S. Lee, *J. Chem. Phys.* **107**, 2734 (1997).
- [17] R. D. Levine, *Quantum Mechanics of Molecular Rate Processes* (Clarendon Press, Oxford, 1969), p. 191.
- [18] T. Seideman, *J. Chem. Phys.* (to be published).
- [19] U. Fano, *Phys. Rev.* **124**, 1866 (1961).
- [20] J. J. Sakurai, *Modern Quantum Mechanics* (Addison-Wesley, Reading, 1994).
- [21] S. A. Reid, J. T. Brandon, and H. Reisler, *J. Phys. Chem.* **97**, 540 (1993).
- [22] T. Nakajima and P. Lambropoulos, *Phys. Rev. Lett.* **70**, 1081 (1993); *Phys. Rev. A* **50**, 595 (1994).